# Identification and analysis of a bottleneck in PCB biodegradation

Shaodong Dai[1,2], Frédéric H. Vaillancourt[2–4], Halim Maaroufi[4], Nathalie M. Drouin[4], David B. Neau[1], Victor Snieckus[5], Jeffrey T. Bolin[1] and Lindsay D. Eltis[3,4]

*[1]Markey Center for Structural Biology, Department of Biological Sciences, Purdue University, West Lafayette, Indiana 47907-1392, USA. [2]These authors contributed equally to this work. [3]Departments of Microbiology and Biochemistry, University of British Columbia, Vancouver, British Columbia, V6T 1Z3, Canada. [4]Department of Biochemistry, Pavillon Marchand, Université Laval, Quebec City, Quebec, G1K 7P4, Canada. [5]Department of Chemistry, Queen's University, Kingston, Ontario, K7L 3N6, Canada.*

Published online 4 November 2002; corrected 11 November 2002 (details online); doi:10.1038/nsb866



**The microbial degradation of polychlorinated biphenyls (PCBs) provides the potential to destroy these widespread, toxic and persistent environmental pollutants. For example, the four-step upper *bph* pathway transforms some of the more than 100 different PCBs found in commercial mixtures and is being engineered for more effective PCB degradation. In the critical third step of this pathway, 2,3-dihydroxybiphenyl (DHB) 1,2-dioxygenase (DHBD; EC 1.13.11.39) catalyzes aromatic ring cleavage. Here we demonstrate that *ortho*-chlorinated PCB metabolites strongly inhibit DHBD, promote its suicide inactivation and interfere with the degradation of other compounds. For example, $k_{cat}^{app}$ for 2′,6′-diCl DHB was reduced by a factor of ~7,000 relative to DHB, and it bound with sufficient affinity to competitively inhibit DHB cleavage at nanomolar concentrations. Crystal structures of two complexes of DHBD with *ortho*-chlorinated metabolites at 1.7 Å resolution reveal an explanation for these phenomena, which have important implications for bioremediation strategies.**

The potential benefits of improved biodegradation of polychlorinated biphenyls (PCBs) motivate studies of the structure and function of the four enzymes of the bacterial *bph* pathway, which transforms biphenyl to benzoate and 2-hydroxypenta-2,4-dienoate[1]. PCB degradation is complicated because PCBs are produced and distributed as complex mixtures[2]. The range of PCBs transformed by the pathway is highly dependent upon the bacterial strain. Some strains do not transform PCBs that contain more than three chlorines, whereas other strains, such as *Burkholderia* sp. LB400, transform up to hexachlorinated biphenyls[3]. This variation has been studied extensively in terms of biphenyl dioxygenase, the first *bph* pathway enzyme, with the ultimate goal of improving the biodegradation of PCBs. For biphenyl dioxygenase, directed mutagenesis and directed evolution have helped identify determinants of substrate selectivity and increase substrate range[4,5]. Although the capabilities of the remaining *bph* pathway enzymes are less thoroughly characterized, it is clear that other steps in the pathway can limit the degradation of particular PCBs[6–8].

DHBD (2,3-dihydroxybiphenyl 1,2-dioxygenase), the third enzyme of the *bph* pathway, is of particular significance in the degradation of PCBs because it is incapable of transforming certain chlorinated DHBs (2,3-dihydroxybiphenyl)[6,7] and is subject to various types of inhibition, as well as suicide inactivation[9,10].

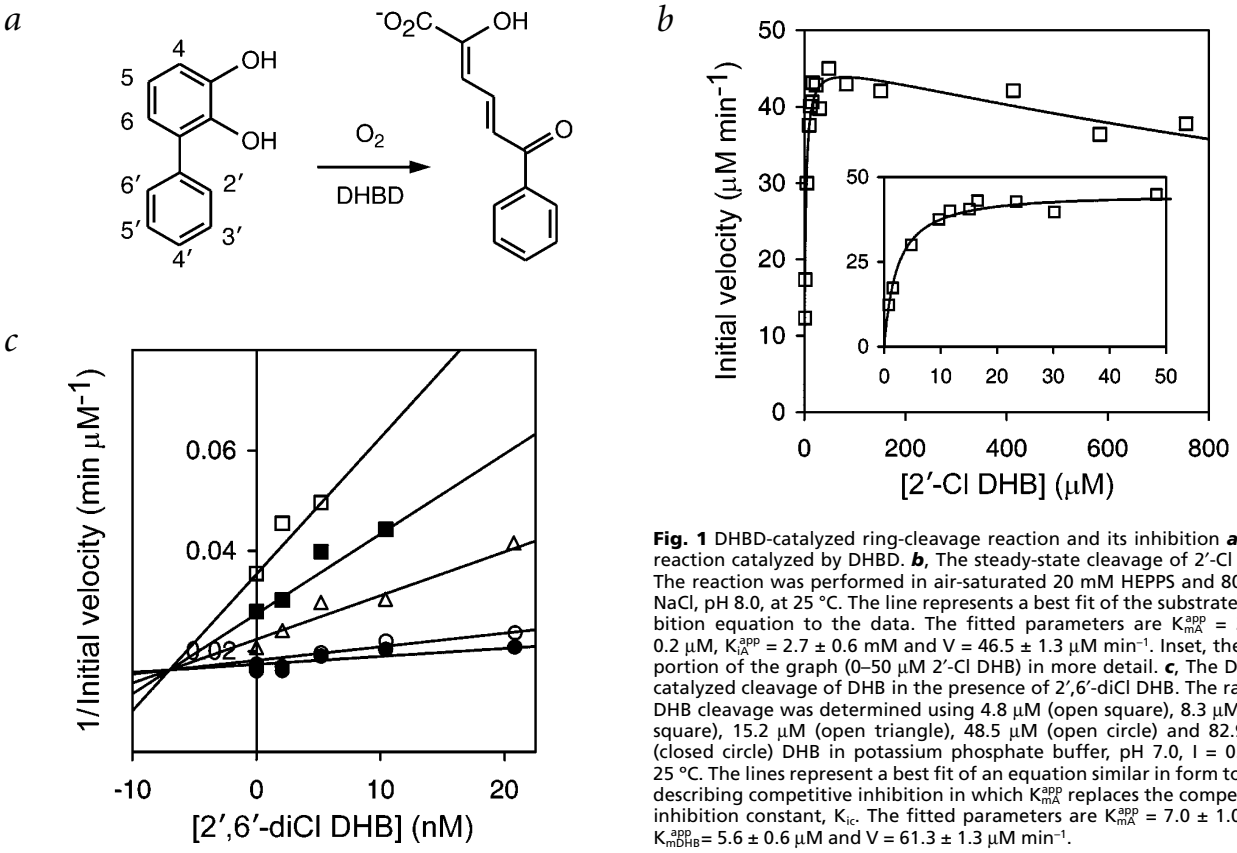


**Fig. 1** DHBD-catalyzed ring-cleavage reaction and its inhibition ***a***, The reaction catalyzed by DHBD. ***b***, The steady-state cleavage of 2′-Cl DHB. The reaction was performed in air-saturated 20 mM HEPPS and 80 mM NaCl, pH 8.0, at 25 °C. The line represents a best fit of the substrate inhibition equation to the data. The fitted parameters are $K_{mA}^{app}$ = 2.3 ± 0.2 μM, $K_{iA}^{app}$ = 2.7 ± 0.6 mM and V = 46.5 ± 1.3 μM min$^{-1}$. Inset, the first portion of the graph (0–50 μM 2′-Cl DHB) in more detail. ***c***, The DHBD-catalyzed cleavage of DHB in the presence of 2′,6′-diCl DHB. The rate of DHB cleavage was determined using 4.8 μM (open square), 8.3 μM (full square), 15.2 μM (open triangle), 48.5 μM (open circle) and 82.9 μM (closed circle) DHB in potassium phosphate buffer, pH 7.0, I = 0.1, at 25 °C. The lines represent a best fit of an equation similar in form to that describing competitive inhibition in which $K_{mA}^{app}$ replaces the competitive inhibition constant, $K_{ic}$. The fitted parameters are $K_{mA}^{app}$ = 7.0 ± 1.0 nM, $K_{mDHB}^{app}$ = 5.6 ± 0.6 μM and V = 61.3 ± 1.3 μM min$^{-1}$.

**Table 1 Steady-state kinetic and inactivation parameters of DHBD for chlorinated DHBs[1]**

| Compound | DHB[2] | 2′-Cl DHB | 3′-Cl DHB | 4′-Cl DHB | 4-Cl DHB | 5-Cl DHB | 6-Cl DHB | 2′,6′-diCl DHB[3] |
|---|---|---|---|---|---|---|---|---|
| $K_{dA}$ (μM) | 8 (1) | 0.8 (0.6) | 8.4 (4.6) | 52.7 (6.3) | 9.0 (2.2) | 9.4 (3.2) | 9.2 (0.8) | – |
| $K_{mA}$ (μM) | 22 (2) | 8.9 (1.8) | 126 (16) | 47 (6) | 41 (14) | 45 (4) | 6.1 (0.6) | 0.007 (0.001) |
| $K_{iA}$ (mM) | 3.0 (0.5) | 2.75 (0.64) | 0.270 (0.005) | 0.224 (0.002) | – | 1.5 (0.2) | 0.29 (0.03) | – |
| $K_{mB}$ (μM) | 1,280 (70) | 1,550 (160) | 513 (78) | 329 (55) | 1,190 (320) | 468 (34) | 104 (13) | – |
| $k_{cat}$ ($s^{-1}$) | 1,350 (110) | 33 (5) | 790 (120) | 850 (120) | 278 (59) | 164 (11) | 53 (2) | 0.036 (0.001) |
| $k_A$ ($\times 10^6$ $M^{-1}s^{-1}$) | 62 (8) | 3.7 (0.8) | 6.3 (0.5) | 17.9 (2.7) | 6.8 (1.2) | 3.7 (0.4) | 8.8 (1.0) | 5.1 (0.9) |
| $k_B$ ($\times 10^6$ $M^{-1}s^{-1}$) | 1.0 (0.1) | 0.0212 (0.0012) | 1.5 (0.2) | 2.6 (0.6) | 0.24 (0.02) | 0.35 (0.03) | 0.52 (0.07) | – |
| Partition ratio | 84,900 (1,400) | 1,390 (150) | 42,000 (14,000) | 40,600 (5,500) | 10,850 (400) | 12,000 (1,500) | 5,500 (470) | 49.5 (1.6) |
| $k_{inact}^{app}$ ($\times 10^{-3}$ $s^{-1}$)[4] | 3.0 (0.1) | 3.6 (0.9) | 7.3 (2.9) | 10.6 (2.7) | 6.6 (0.3) | 5.2 (0.9) | 7.0 (0.8) | 0.69 (0.01) |
| $k_{inact}^{app}$ / $K_{mA}^{app}$ ($\times 10^3$ $M^{-1}s^{-1}$) | 0.25 (0.10) | 1.6 (0.5) | 0.13 (0.06) | 0.16 (0.07) | 0.29 (0.06) | 0.20 (0.06) | 1.1 (0.2) | 99 (16) |

[1] $K_{dA}$, $K_{mA}$, $K_{iA}$, $k_A$ and $k_{inact}^{app}$ represent the dissociation constant, $K_m$, inhibition constant, specificity constant and the apparent rate constant of inactivation during catalytic turnover in air-saturated buffer, respectively, for DHB or Cl-DHBs. $K_{mB}$ and $k_B$ represent the $K_m$ and specificity constant for $O_2$. The partition ratio, $k_{inact}^{app}$ and $k_{inact}^{app}$ / $K_{mA}^{app}$ were determined in air-saturated buffer. Values in parentheses are standard errors.
[2] Part of the data was taken from ref. 9.
[3] The parameters for 2′,6′-diCl DHB are all apparent parameters obtained in air-saturated buffer.
[4] $k_{inact}^{app}$ was calculated by dividing $k_{cat}^{app}$, the apparent $k_{cat}$ obtained in air-saturated buffer, by the partition ratio (equation 2 in ref. 10), except for 2′,6′-diCl DHB where $k_{inact}^{app}$ was determined spectrophotometrically (equations 3 and 4 in ref. 10).

DHBD is an extradiol dioxygenase and uses mononuclear non-heme iron(II) to cleave DHB (Fig. 1*a*). Extradiol dioxygenases use an ordered, ternary complex mechanism in which the catecholic substrate binds first to the active site Fe(II) in a bidentate manner, activating the ferrous center for binding of $O_2$ (reviewed in ref. 11). Suicide inhibition of DHBD in the presence of DHB or 3-chlorocatechol involves release of superoxide from the DHBD–DHB–$O_2$ ternary complex and oxidation of the active site Fe(II)[10]. To gain insight into the PCB-transforming capabilities of DHBD, we investigated the specificity of the enzyme for a series of chlorinated DHBs, as well as the involvement of inhibition and inactivation as limiting factors *in vitro* and *in vivo*. The results of these studies revealed that *ortho*-chlorinated DHBs are potent and physiologically significant inhibitors of DHBD and motivated crystallographic studies of the structural basis for the observed patterns of reactivity.

## The DHBD-catalyzed cleavage of chlorinated DHBs

The specificity of DHBD for chlorinated DHBs and the susceptibility of the enzyme to inactivation during cleavage of these compounds were investigated. Kinetic experiments performed by varying the concentration of monochlorinated DHBs and $O_2$ (Table 1) showed that DHBD cleaved the chlorinated DHBs with specificities 0.06×–0.3× those of unchlorinated DHB in the following order: DHB > 4′-Cl > 6-Cl > 4-Cl > 3′-Cl > 5-Cl ≈ 2′-Cl DHB. Interestingly, the $K_m$ of DHBD for $O_2$ was lower in the presence of 5-Cl, 6-Cl, 3′-Cl and 4′-Cl DHB than unchlorinated DHB. In addition, the specificity constant for $O_2$, $k_B$, varied in the presence of the DHBs by >100-fold in the following order: 4′-Cl > 3′-Cl > DHB > 6-Cl > 5-Cl > 4-Cl > 2′-Cl DHB.

The most significant findings pertain to the most slowly cleaved monochlorinated DHB, 2′-Cl DHB, for which DHBD had a high affinity (low $K_d$) and a 50-fold decrease in specificity for $O_2$, relative to DHB. These results led to the synthesis of 2′,6′-diCl DHB and the study of its cleavage. Steady-state cleavage of 2′,6′-diCl DHB was too slow for the standard dioxygen consumption assay. However, by using DHB as a reporter substrate, DHBD was shown to have a $K_{mA}^{app}$ = 7 ± 1 nM for 2′,6′-diCl DHB in air-saturated buffer, which is significantly lower than for 2′-Cl DHB (Fig. 1*b*,*c*; Table 1).

The susceptibility of DHBD to inactivation during cleavage of chlorinated DHBs was evaluated by determining $k_{inact}^{app}$, the apparent rate constant for inactivation during catalytic turnover. Based on $k_{inact}^{app}$/ $K_{mA}^{app}$, DHBD was inactivated in the following order of efficiency: 2′,6′-diCl > 2′-Cl > 6-Cl > 4-Cl > DHB > 5-Cl > 4′-Cl > 3′-Cl DHB. 2′,6′-diCl DHB and 2′-Cl DHB inactivated DHBD ~400× and 6× more efficiently than DHB, respectively, (Table 1) primarily because of their low $K_{mA}^{app}$. However, in the presence of saturating concentrations of individual substrates, DHBD was inactivated in the following order: 4′-Cl > 3′-Cl > 6-Cl > 4-Cl > 5-Cl > 2′-Cl > DHB > 2′,6′-diCl DHB.

## Consequences of *in vitro* inactivation of DHBD

Inactivation of DHBD during cleavage of 3-chlorocatechol and nonchlorinated catechols involves oxidation and loss of the active site iron, probably *via* dissociation of superoxide from the enzyme–substrate–$O_2$ ternary complex[10]. To investigate whether chlorinated DHBs inactivate DHBD in a similar fashion, the enzyme was inactivated using 4-Cl, 2′-Cl and 2′,6′-diCl DHB. DHBD could be partially reactivated to 10 ± 1 and 12 ± 1% of its initial activity for 4-Cl and 2′-Cl DHB, respectively, through anaerobic incubation with the reducing agent dithiothreitol (DTT). Incubation with Fe(II) and DTT was necessary to restore 84 ± 6 and 71 ± 7% of the initial activity for 4-Cl and 2′-Cl DHB, respectively. As determined by mass spectrometry, preparations of inactivated DHBD had molecular masses identical to active DHBD, indicating that DHBD was not covalently modified during mechanism-based inactivation. Investigation of a sample of 2′,6′-diCl DHB-inactivated enzyme by EPR spectroscopy revealed the presence of ferric iron (g = 4.3) in an amount corresponding to the quantity of DHBD in the sample. Thus, the $O_2$-dependent inactivation of DHBD in presence of chlorinated DHBs is similar to that described for other catecholic substrates[10].

**Table 2 Distances from active site Fe to nearest atoms**

| Substrate | Distance (Å) to atom[1] | | | | | |
|---|---|---|---|---|---|---|
| | H146 Nε2 | H210 Nε2 | E260 Oε1 | DHB O2 | DHB O3 | Water |
| DHB | 2.2 | 2.3 | 2.0 | 2.0 | 2.4 | 2.4 |
| 2′-Cl DHB | 2.3 | 2.3 | 2.0 | 2.1 | 2.3 | 2.4 |
| 2′,6′-diCl DHB | 2.2 | 2.3 | 2.2 | 2.2 | 2.4 | 2.6 |

[1]DHB O2 and DHB O3 refer to the 2- and 3-oxo/hydroxo substituents of DHB and Cl-DHBs.

### *In vivo* inhibition

To determine whether inhibition of DHBD by 2′,6′-diCl DHB is physiologically relevant, the *in vivo* inhibition of the enzyme was studied using the native strain of the enzyme, *Burkholderia* sp. LB400, and a heterologous expression host, *Escherichia coli* DH5α. The activity of DHBD in biphenyl-grown *Burkholderia* sp. LB400 and LB-grown *E. coli* DH5α was 0.3 and 0.2 U $OD_{600}^{-1}$, respectively. Addition of 80 μM 2′,6′-diCl DHB to the assay completely inhibited DHBD activity in both strains. Upon removal of 2′,6′-diCl DHB from the cells, the activity of DHBD in *Burkholderia* sp. LB400 and in *E. coli* DH5α was 123 ± 1 and 87.5 ± 0.5%, respectively, when compared with the activity of controls in which the cells were incubated with DHB but not with 2′,6′-diCl DHB. This recovery of activity occurred in the presence of chloramphenicol, indicating protein synthesis is not required.

The *in vivo* inhibition of DHBD by 2′,6′-diCl DHB is consistent with the failure to observe a ring-cleavage product when *Burkholderia* sp. LB400 was incubated in the presence of 2,6-diCl biphenyl[7]. Moreover, although *Burkholderia* sp. LB400 transforms *ortho*-chlorinated congeners relatively well, it transformed <5% of 2,6-diCl biphenyl to the corresponding benzoate, compared with >70% for other congeners[12]. To test whether catabolism of 2,6-diCl biphenyl inhibits the *bph* pathway, we evaluated the effect of this congener on growth rates of *Burkholderia* sp. LB400 at different stages during growth on biphenyl. Growth was monitored as the change in optical density at 600 nm. During early log phase, cells grew on biphenyl at a rate of 0.061 ± 0.005 $h^{-1}$. At the corresponding culture time, cells growing on a mixture of biphenyl and 2,6-diCl biphenyl did so at a rate of 0.010 ± 0.001 $h^{-1}$. At mid log phase, cells grew on biphenyl at a rate of 0.205 ± 0.004 $h^{-1}$. At the corresponding culture time, cells on the mixture grew at a rate of 0.041 ± 0.004 $h^{-1}$. Thus, 2,6-diCl biphenyl inhibited growth of *Burkholderia* sp. LB400 on biphenyl 5–6 fold.

### Structures of DHBD in complex with *ortho*-Cl DHBs

Crystal structures of anaerobic, binary complexes of DHBD with 2′-Cl DHB and 2′,6′-diCl DHB were analyzed at 1.7 Å resolution. As expected, the structures of both complexes are approximately isomorphous with structures of the substrate-free enzyme (PDB entry 1HAN)[13] and the enzyme–DHB complex (PDB entry 1KMY)[9,14].

For both Cl-DHB complexes initial electron density maps showed readily interpretable density for the active site Fe atoms, one water ligand and the Cl-DHBs. Modeling and refinement of both structures was straightforward. The Fe is bound by three protein ligands, His 146, His 210 and Glu 260, as observed for the substrate-free enzyme[13] and various enzyme–substrate complexes[9,15,16]. 2′-Cl DHB and 2′,6′-diCl DHB each bind to the Fe through both hydroxyl substituents, as observed in enzyme–substrate complexes[9,15,16]. Several lines of evidence, including the distances between Fe and the oxo/hydroxo substituents, indicate that DHB binds as a monoanion, with the 2-OH group deprotonated[14,16]. Both complexes reported here are consistent with this model (Table 2). As in the DHB complex, a water molecule binds near the Fe and occupies the probable $O_2$-binding site *trans* to Glu 260. The isotropic B-values of this water molecule in the three complexes are 21–26 $Å^2$, suggesting approximately equivalent occupancy.

The Cl-DHBs occupy essentially the same space in the active site and their equivalent atoms interact similarly with the protein. All atoms in the hydroxylated rings of the Cl-DHBs superimpose to within 0.15 Å, whereas positional differences between atoms in the chlorinated rings reach 0.3–0.4 Å for atoms C3′, C4′ and C5′. These variations do not arise from a significant difference in conformation but from a small difference in overall orientation associated with contacts between the 6′-Cl substituent of the dichlorinated compound and side chain atoms of His 241, Tyr 250 and Pro 280. Only a few protein atoms in two side chains in contact with C3′, C4′ and C5′ move by >0.3 Å and none move by >0.5 Å. In summary, the Cl-DHBs bind in the same manner without requiring significant changes in protein structure.

Thus, the most compelling result is the consistent placement of the 2′-Cl substituent near the $O_2$-binding site in both complexes (Fig. 2). In both complexes, the 2′-Cl atom makes nonbonded contacts at distances of 3.5–3.9 Å with side chain atoms of conserved residues Val 148 and Phe 187, which are presumed to contribute to the $O_2$-binding pocket. The Cl is also near the water that occupies the proposed $O_2$-binding site; the distance to the water oxygen is 3.6 Å in the 2′-Cl DHB complex and 3.3 Å in the 2′,6′-diCl DHB complex. Slight variations in the positions of the Cl atoms (0.15 Å) and the water molecules (0.19 Å) between the two complexes seem to contribute equivalently to the net difference.

It is reasonable to expect that the site occupied by the 6′-Cl substituent of 2′,6′-diCl DHB would be partially occupied by the Cl substituent of 2′-Cl DHB. However, throughout the refinement, difference density maps provided no compelling evidence of this second binding mode. In the final ($F_o - F_c$) map, positive density of significant volume is not observed until the contour level is lowered to 1.5 σ, where σ is the standard deviation from a mean of zero. In comparison, density of comparable volume is observed at 3σ for unmodeled alternative locations of Oγ of Ser 236, Oγ of Ser 279 and Cε of Met 212.

Comparisons between the Cl-DHB complexes and the DHB complex (Fig. 2*b*) demonstrate differences in the overall orientation of the substrates and a difference in conformation, which seems to arise from the presence or absence of a 2′-Cl substituent. The net result is differences of up to 1.1 Å in the positions of equivalent atoms in the nonhydroxylated rings. Typical positional differences for protein atoms are smaller, such that only a few side chain atoms of residues in contact with the nonhydroxylated ring differ in position by >0.3 Å. Only one atom, Cε of Met 175, which is in contact with the distal ring, moves by >0.5 Å in association with a change in $\chi^3$.

The crystal structures of the DHBD–2′-Cl DHB and DHBD–2′,6′-diCl DHB complexes rationalize the distinguishing reactivities of these substrates. In both cases, the 2′-Cl substituent binds in contact with conserved side chains that are believed to define the $O_2$-binding site and with a water molecule that occupies that site in the absence of $O_2$. These interactions likely contribute to the factor of 10 reduction in $K_d$ observed for 2′-Cl DHB in comparison to DHB. In addition, for both compounds, the 2′-Cl substituent has the potential to partially inhibit binding of $O_2$ to the binary complex and/or affect the

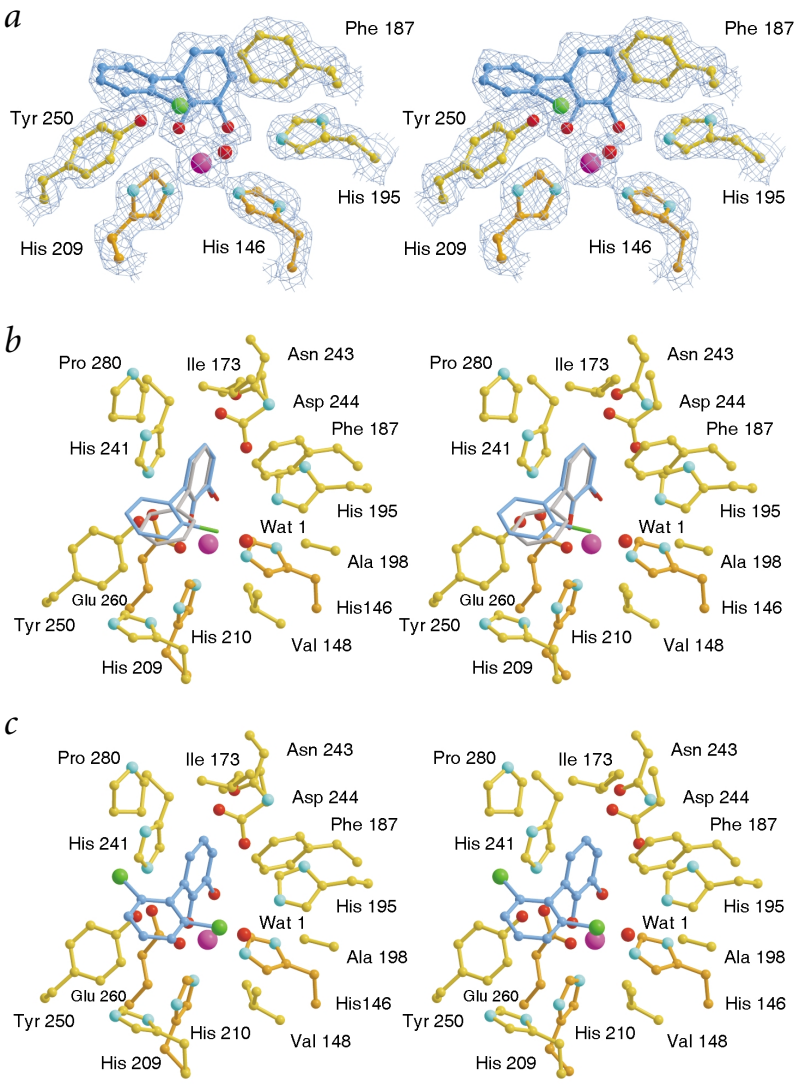


**Fig. 2** Illustrations of *ortho*-chlorinated DHBs bound to the active site of DHBD. ***a***, Stereo view of $(2F_o - F_c)\ \exp(i\alpha_c)$ electron density (1.7 Å resolution and 1.5 σ) in the vicinity of 2′-Cl DHB and some nearby side chains of DHBD. For 2′-Cl DHB, C, Cl and O atoms are blue, green and red, respectively. For DHBD, C, N and O atoms are yellow, cyan and red. Side chains with orange carbon atoms are ligands of the Fe atom, which is the larger magenta sphere. ***b***, Stereo view of DHB superimposed on the structure of the 2′-Cl DHBD–DHB complex. The coordinates for DHB were obtained by least squares superposition of the Cα atoms for residues 140–280 from the two complexes using the structure of 2′-Cl DHB as the reference. The color scheme is the same as in panel (*a*). For 2′-Cl DHB and DHB, the carbon atoms are blue and gray, respectively. Two side chains that contact the chlorinated ring in the foreground are not shown. Met 175 sits above the ring adjacent to Pro 280, and the outer edge of Phe 202 approaches atom C3′ from above and between His 209 and Val 148. ***c***, 2′,6′-diCl DHB bound to the active site of DHBD. The view and color scheme are the same as in panel (*b*).

orientation of the bound $O_2$ relative to the Fe and the point of attack on the hydroxylated ring of the substrate. One likely consequence is inefficient catalysis, as reflected in the appreciably reduced values of $k_{cat}$. Moreover, contact between $O_2$ and the Cl substituent could bias the orientations available to $O_2$ away from those competent for the cleavage reaction without prohibiting reduction of $O_2$ or dissociation of superoxide. This scenario would explain why the Cl substituent does not reduce the rate of inactivation within the ternary complex to the same extent that it reduces $k_{cat}$.

For 2′,6′-diCl DHB, $k_{cat}^{app}$ and $K_{mA}^{app}$ are reduced by factors of 7,000 and 1,700 relative to DHB, such that $k_{cat}^{app} / K_{mA}^{app}$ is only 4-fold lower. These almost parallel effects on $k_{cat}^{app}$ and $K_{mA}^{app}$ suggest nonproductive binding of 2′,6′-diCl DHB. In the case of 2′-diCl DHB, $k_{cat}^{app}$ and $K_{mA}^{app}$ are reduced relative to DHB by smaller factors of 50 and 5.2, respectively, such that $k_{cat}^{app} / K_{mA}^{app}$ is 10-fold lower. The differences between $k_{cat}^{app}$, $K_{mA}^{app}$ and $k_{cat}^{app} / K_{mA}^{app}$ for the two Cl-DHBs suggest that 2′-Cl DHB can more readily assume the productive binding mode. This is consistent with the crystal structures inasmuch as the orientation and conformation of 2′,6′-diCl DHB are more restricted because of contacts between the 6′-Cl substituent and the enzyme.

## Conclusions

*Ortho*-chlorinated PCB congeners elicit a wide range of toxic responses and are among the most recalcitrant to chemical and biological remediation. Although health concerns have focused on the non-*ortho* substituted, or 'dioxin-like', congeners, more recent studies have demonstrated that the *ortho*-substituted congeners are neurotoxic[17] and tumor-promoting[18], and elicit endocrine changes[19]. Moreover, *ortho*-substituted congeners are poorly destroyed by various chemical[20,21] and biological treatments[2]. One of the most promising biological treatments consists of sequential anaerobic-aerobic treatment[2]. Unfortunately, most consortia of anaerobic bacteria preferentially catalyze the *meta*- and *para*-dehalogenation of PCBs, yielding mixtures of predominantly *ortho*-chlorinated congeners[22]. Moreover, such congeners are poorly transformed by aerobic PCB-degrading bacteria[2,12,23,24]. Strains that aerobically degrade *ortho*-chlorinated congeners would be useful whether used alone to remediate environments contaminated with lightly chlorinated congeners or in conjunction with other treatments to remediate environments contaminated with highly chlorinated congeners. Identification of 2′,6′-diCl DHB as a metabolite with a high affinity for DHBD that inactivates the enzyme not only identifies a metabolic block but also suggests strategies to overcome it. In particular, directed evolution of DHBD to either improve its ability to cleave 2′,6′-diCl DHB or to decrease its affinity for this compound should enhance the utility of bacterial strains for aerobic biodegradation of PCBs.

## Methods

**Chemicals, strains and growth.** DHB, 4-Cl, 5-Cl, 6-Cl, 2′-Cl, 3′-Cl, 4′-Cl and 2′,6′-diCl DHB[25], as well as 2,6-diCl biphenyl (S. Nerdinger, C. Kendall, R. Marchart, P. Riebel, M.R. Johnson, C.-F. Yin, N. Haenaff, L.D.E. and V.S., in preparation), were synthesized according to established procedures. DHBD was overexpressed in *Pseudomonas putida* KT2442 as described[9]. *Burkholderia* sp. LB400 and *E. coli* DH5α that contained plasmid pLEBD4 were cultured as described[10].

**Table 3 Crystallographic data and refinement statistics**

| DHBD complex | 2′-Cl DHB | 2′,6′-diCl DHB |
|---|---|---|
| Space group (Z) | I422 (16) | I422 (16) |
| Unit cell dimensions (Å) | | |
| a = b | 122.337 | 122.640 |
| c | 106.947 | 107.232 |
| Resolution range (Å) | 50.00–1.69 | 50.00–1.69 |
| Reflections | | |
| Unique | 44,042 | 46,029 |
| Total | 1,480,972 | 2,212,442 |
| Completeness (%)[1] | 96.8 (94.8) | 90.2 (73.7) |
| $R_{merge}$[1,2] | 0.083 (0.340) | 0.086 (0.409) |
| Refinement range (Å) | 25.0–1.7 | 25.0–1.7 |
| R-factor, reflections[3] | 0.212, 43,300 | 0.212, 40,299 |
| $R_{free}$, reflections[3] | 0.241, 2,170 | 0.231, 2,012 |
| R.m.s. deviation from restraints | | |
| Bond lengths (Å) | 0.0063 | 0.0062 |
| Bond angles (Å) | 1.27 | 1.27 |
| Average atomic B-values (Å$^2$) | | |
| Protein | | |
| Main chain | 20.7 | 18.9 |
| Side chain | 22.7 | 21.6 |
| Fe | 18.6 | 26.2 |
| Cl-DHBs | 22.6 | 23.0 |
| Water | 37.5 | 36.5 |

[1]Number in parentheses is for the last shell (1.75–1.69 Å).
[2]$R_{merge} = \Sigma_h\Sigma_i |I_i(h) - \langle I(h)\rangle| / \Sigma_h\Sigma_i I_i(h)$, where $I_i(h)$ is one measurement of the intensity of reflection h, and $\langle I(h)\rangle$ is the mean of all such measurements.
[3]R-factor = $\Sigma_h |F_o(h) - F_c(h)| / \Sigma_h F_o(h)$, where $F_o(h)$and $F_c(h)$ are observed and calculated structure factor amplitudes. The sums include all reflections against which the model was refined (working set). $R_{free}$ is defined by the same equation, but the sums include reflections omitted from the refinement (test set).

**Preparation of DHBD samples.** DHBD samples were anaerobically purified and handled essentially as described[9,10]. For crystallographic studies, DHBD was further purified using hydrophobic interaction chromatography (M.I. Davis, E.C. Wasinger, A. Decker, M.Y.M. Pau, F.H.V., J.T.B., L.D.E., B. Hedman, K.O. Hodgson and E.I. Solomon, in preparation).

**Kinetic and mechanism-based inactivation studies.** Enzymatic activity was routinely measured by following consumption of $O_2$ using a Clark-type polarographic $O_2$ electrode (Yellow Springs Instruments) and analyzed as described[9]. All experiments were performed using 20 mM 4-(2-hydroxyethyl)-1-piperazinepropanesulfonic acid (HEPPS) and 80 mM NaCl, pH 8.0, at 25.0 ± 0.1 °C (290 μM dissolved $O_2$) unless otherwise stated. The parameters of all steady-state rate equations were analyzed using the least squares and dynamic weighting options of Leonora[26].

Specificity was investigated essentially as described[9]. Apparent steady-state parameters for the cleavage of 2′,6′-diCl DHB by DHBD were determined using DHB as a reporter substrate in the $O_2$ consumption assay (potassium phosphate buffer, pH 7.0 (I = 0.1)). Concentrations of DHB and 2′,6′-diCl DHB were varied from 5 to 85 μM (concentrations at which substrate inhibition was negligible) and from 2.1 to 20.9 nM, respectively. An equation identical in form to that for competitive inhibition was fit to the data[26]. In this equation, $K_m^{app}$ of 2′,6′-diCl DHB replaces the competitive inhibition constant, $K_{ic}$.

Partition ratios expressing the number of substrate molecules consumed per enzyme molecule inactivated were determined for most substrates using a dioxygen consumption assay[10]. For 2′,6′-diCl DHB, the partition ratio was determined spectrophotometrically by following the appearance of the ring-cleaved product ($\lambda_{max}$ = 391 nm, potassium phosphate buffer, pH 7.0 (I = 0.1), ε = 36.5 $mM^{-1}cm^{-1}$).

For most substrates, the apparent rate constant of inactivation during catalytic turnover in air-saturated buffer, $k_{inact}^{app}$ (parameter $j_3^{app}$ of equations 3 and 4 in ref. 10), was calculated from partition ratios determined under saturating substrate conditions ([S] >> $K_m$) (equation 2 in ref. 10). For 2′,6′-diCl DHB, $k_{inact}^{app}$ was assessed from progress curves obtained from the spectrophotometric assay performed at several concentrations of 2′,6′-diCl DHB (100–200 μM) (equations 3 and 4 in ref. 10). The apparent catalytic constant for 2′,6′-diCl DHB, $k_{cat}^{app}$, was determined using the initial velocities of these same assays as they were performed under saturating substrate concentrations.

***In vitro* inactivation and reactivation of DHBD.** *In vitro* inactivation of DHBD with 4-Cl DHB and 2′-Cl DHB, enzyme reactivation, ion-spray mass spectral analyses and EPR spectroscopy of DHBD inactivated with 2′,6′-diCl DHB were performed as described[10].

***In vivo* inhibition studies.** *Burkholderia* sp. LB400 was grown on 2% (w/v) biphenyl, and on 2% biphenyl containing 50 μM 2,6-diCl biphenyl. Growth was monitored at 600 nm. DHBD activity assays were performed using biphenyl-grown *Burkholderia* sp. LB400 and LB-grown *E. coli* DH5α containing the plasmid pLEBD4 as described[10]. DHBD activity was inhibited using 80 μM 2′,6′-diCl DHB. Cells were washed and re-assayed for DHBD as described[10].

**Crystallization and preparation of complexes.** Crystals of substrate-free enzyme were grown anaerobically at 10 °C under conditions similar to those reported[13]. Before exposure to Cl-DHBs, the apparatus was equilibrated for at least 4 h at 20 °C. Crystals were then serially transferred through solutions containing 10% (v/v) *t*-butanol, 100 mM HEPES buffer, pH 7.0, 10 mM ferrous ammonium sulfate, and successively higher concentrations (for example, 25%, 27% and 30% (v/v)) of PEG 400. Complexes were prepared by incubating crystals overnight at 20 °C in solutions (10 μl) containing 30% (v/v) PEG 400, 10% (v/v) *t*-butanol, 30 mM Cl-DHBs, 100 mM HEPES buffer, pH 7.0, and 10 mM ferrous ammonium sulfate. Crystals were flash-frozen in liquid $N_2$ inside the glove box.

**Diffraction experiments and structure analysis.** Diffraction patterns were acquired at beamline 19-ID of the Advanced Photon Source. The X-ray wavelength was 0.97833 Å, and crystals were maintained at temperatures of 105–110 K. Diffractions patterns were analyzed using HKL2000 (ref. 27). Rigid-body refinement using REFMAC[28] from the CCP4 package[29] established an initial model consisting of the substrate-free structure (PDB code 1HAN[13]) with the active site Fe atom and nearby water molecules deleted. Data collection and refinement statistics are summarized in Table 3. CNS[30] was used for subsequent refinement and calculation of electron density maps. O[31] was used to evaluate the maps and build models. QUANTA (Molecular Simulations, Inc.) was used to construct atomic structures of Cl-DHBs. MolScript[32], BobScript[33] and Raster3D[34] were used to create figures illustrating atomic models and electron density maps.

**Coordinates.** Coordinates and structure factors were deposited in the Protein Data Bank (accession code 1LGT for the DHBD–2′Cl DHB and 1LKD for the DHBD–2′,6′-diCl DHB complexes).

**Acknowledgments**
This research was supported by a Strategic grant from the Natural Sciences and Engineering Research Council of Canada (NSERC) and an award from the U.S. National Institutes of Health (NIH). Use of the Argonne National Laboratory Structural Biology Center beamlines at the Advanced Photon Source was supported by the U. S. Department of Energy, Office of Biological and Environmental Research. F.H.V. was the recipient of an NSERC postgraduate scholarship. D.B.N. was supported in part by an NIH institutional training award. S. He, G. Labbé and W. Minor are thanked for their expert assistance.

**Competing interests statements**
The authors declare that they have no competing financial interests.

Correspondence should be addressed to J.T.B. *email: jtb@purdue.edu* or L.D.E. *email: leltis@interchange.ubc.ca*

Received 29 July, 2002; accepted 1 October, 2002.

1. Furukawa, K. *Curr. Opin. Biotechnol.* **11**, 244–249 (2000).
2. Abramowicz, D.A. *Crit. Rev. Biotechnol.* **10**, 241–251 (1990).
3. Bopp, L.H. *J. Ind. Microbiol.* **1**, 23–29 (1986).
4. Suenaga, H., Watanabe, T., Sato, M., Ngadiman & Furukawa, K. *J. Bacteriol.* **184**, 3682–3688 (2002).
5. Barriault, D., Plante, M.M. & Sylvestre, M. *J. Bacteriol.* **184**, 3794–3800 (2002).
6. Furukawa, K., Tomizuka, N. & Kamibayashi, A. *Appl. Environ. Microbiol.* **35**, 223–227 (1978).
7. Seeger, M., Timmis, K.N. & Hofer, B. *Appl. Environ. Microbiol.* **61**, 2654–2658 (1995).
8. Seah, S.Y. *et al. J. Biol. Chem.* **275**, 15701–15708 (2000).
9. Vaillancourt, F.H., Han, S., Fortin, P.D., Bolin, J.T. & Eltis, L.D. *J. Biol. Chem.* **273**, 34887–34895 (1998).
10. Vaillancourt, F.H., Labbe, G., Drouin, N.M., Fortin, P.D. & Eltis, L.D. *J. Biol. Chem.* **277**, 2019–2027 (2002).
11. Bugg, T.D.H. & Lin, G. *Chem. Commun. (Camb.)* **11**, 941–952 (2001).
12. Maltseva, O.V., Tsoi, T.V., Quensen, J.F. III, Fukuda, M. & Tiedje, J.M. *Biodegradation* **10**, 363–371 (1999).
13. Han, S., Eltis, L.D., Timmis, K.N., Muchmore, S.W. & Bolin, J.T. *Science* **270**, 976–980 (1995).
14. Vaillancourt, F.H. *et al. J. Am. Chem. Soc.* **124**, 2485–2496 (2002).
15. Uragami, Y. *et al. J. Inorg. Biochem.* **83**, 269–279 (2001).
16. Bolin, J.T. & Eltis, L.D. in *Handbook of Metalloenzymes* (eds Messerschmidt, A., Huber, R., Poulos, T. & Wieghardt, K.) 632–642 (John Wiley & Sons, Chichester; 2001).
17. Chauhan, K.R., Kodavanti, P.R. & McKinney, J.D. *Toxicol. Appl. Pharmacol.* **162**, 10–21 (2000).
18. van der Plas, S.A. *et al*. *Toxicol. Appl. Pharmacol.* **169**, 255–268 (2000).
19. Arcaro, K.F. *et al*. *J. Cell. Biochem.* **72**, 94–102 (1999).
20. Korte, N.E. *et al*. *Waste Manag. (Oxford)* **22**, 343–349 (2002).
21. Weber, R. *et al*. *Chemosphere* **46**, 1255–1262 (2002).
22. Wiegel, J. & Wu, Q. *FEMS Microbiol. Ecol.* **32**, 1–15 (2000).
23. Furukawa, K., Tomizuka, N. & Kamibayashi, A. *Appl. Environ. Microbiol.* **38**, 301–310 (1979).
24. Master, E.R., Lai, V.W., Kuipers, B., Cullen, W.R. & Mohn, W.W. *Environ. Sci. Technol.* **36**, 100–103 (2002).
25. Nerdinger, S. *et al. Chem. Commun. (Camb.)* **22**, 2259–2260 (1999).
26. Cornish-Bowden, A. *Analysis of Enzyme Kinetic Data* (Oxford University Press, Oxford, New York; 1995).
27. Otwinowski, Z. & Minor, W. *Methods Enzymol.* **276**, 307–326 (1997).
28. Murshudov, G.N., Vagin, A.A. & Dodson, E.J. *Acta Crystallogr. D* **53**, 240–255 (1997).
29. Dodson, E.J., Winn, M. & Ralph, A. *Methods Enzymol.* **277**, 620–633 (1997).
30. Brünger, A.T. *et al*. *Acta Crystallogr. D* **54**, 905–921 (1998).
31. Jones, T.A., Zou, J.Y., Cowan, S.W. & Kjeldgaard, M. *Acta Crystallogr. A* **47**, 110–119 (1991).
32. Kraulis, P.J. *J. Appl. Crystallogr.* **24**, 946–950 (1991).
33. Esnouf, R.M. *J. Mol. Graph. Model.* **15**, 132–134 (1997).
34. Merritt, E.A. & Bacon, D.J. *Methods Enzymol.* **277**, 505–524 (1997).